



# OMS-2 nanorod-supported cobalt catalyst for aerobic dehydrocyclization of vicinal diols and amidines: Access to functionalized imidazolones



Feng Xie<sup>a,1,\*</sup>, Xiuwen Chen<sup>a,1</sup>, Xiangyu Zhang<sup>a</sup>, Chujun Luo<sup>a</sup>, Shizhuo Lin<sup>a</sup>, Xiaoyong Chen<sup>a</sup>, Bin Li<sup>a</sup>, Yibiao Li<sup>a</sup>, Min Zhang<sup>a,b,\*</sup>

<sup>a</sup> School of Biotechnology and Health Sciences, Wuyi University, Jiangmen 529020, China

<sup>b</sup> Key Lab of Functional Molecular Engineering of Guangdong Province, School of Chemistry and Chemical Engineering, South China University of Technology, Guangzhou 510641, China

## ARTICLE INFO

### Article history:

Received 8 March 2021

Revised 6 April 2021

Accepted 19 April 2021

Available online 4 May 2021

### Keywords:

Heterogeneous cobalt catalysis

Vicinal diols

Imidazolones

Aerobic dehydrocyclization

## ABSTRACT

The development of reusable base metal catalysts for innovative catalytic transformations is a key technology toward sustainable production of fine chemicals, pharmaceuticals, and other function products. Herein, we report the preparation of a new highly dispersed manganese oxides of octahedral molecular sieve (OMS-2) nanorod-supported cobalt catalyst, which is successfully applied for aerobic dehydrocyclization of vicinal diols and amidines to access structurally diverse imidazolones, a class of valuable compounds found in numerous natural and biomedical products. The developed catalytic transformation proceeds with broad substrate scope, good functional group compatibility, the use of green molecular oxygen and reusable cobalt catalyst, which offers an important platform for the conversion of abundant and sustainable alcohol resources into functional N-heterocycles. The strategy combining nanocatalyst design with aerobic dehydrocoupling is anticipated to achieve other challenging catalytic transformations.

© 2021 Elsevier Inc. All rights reserved.

## 1. Introduction

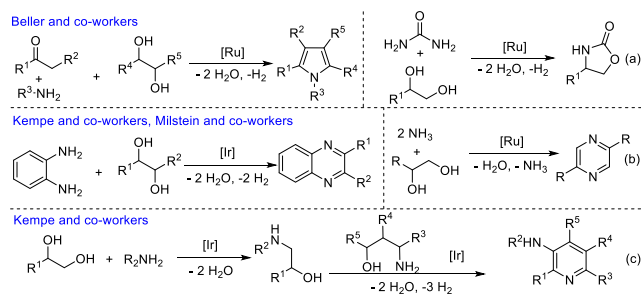
Concerning the energy crisis and gradual deterioration of the ecological environment, it is urgent to find alternatives to traditional petrochemical energy sources as raw materials for the chemical industry [1–3]. As a class of abundant and sustainable resources, vicinal diols are largely produced from fermentation and degradation of lignocellulose in nature [4–5]. Consequently, the search for novel approaches enabling efficient conversion of biomass-derived alcohols into functional products is of significant importance [6–16], and it contributes to reducing CO<sub>2</sub> emissions and conserving our fossil carbon feedstocks. However, due to the existence of two or multiple hydroxy groups, it is hard to control the regioselectivity during the transformation of vicinal diols. Moreover, dehydrogenation-induced activation of diols generally requires elevated temperatures, which easily leads to substrate decomposition [17]. In this context, there is a high demand for the development of compatible catalysts allowing selective conversion of vicinal diols.

Among various functional products, N-heterocycles represent a class of extremely important substances ubiquitously applied in the fields of science and technology [18–20]. However, there are only a handful of examples focusing on the conversion of vicinal diols to N-heterocycles through acceptorless dehydrogenative coupling or hydrogen autotransfer strategy. For instance, Beller and the coworkers have successively reported the synthesis of substituted pyrroles and oxazolidin-2-ones by a ruthenium-catalyzed multi-component reaction and the annulation of vicinal diols with urea, respectively (Scheme 1a) [21–22]. The groups of Kempe and Milstein have successfully converted vicinal diols into quinoxalines/pyrazines with aromatic diamines/ammonia (Scheme 1b) [23–25]. Through initial *mono*-amination of vicinal diols with amines followed by selective dehydrogenative heterocondensation with  $\gamma$ -amino alcohols, Kempe et al demonstrated an iridium-catalyzed *meta*-functionalized pyridines (Scheme 1c) [26]. Despite these interesting catalytic transformations, the utilization of vicinal diols for the construction of imidazolones has never been accomplished. Noteworthy, imidazolones have exhibited a broad spectrum of applications, including the areas of human health [27], drugs [28], bioactive agents [29], metallic ligands [30], fluorescent protein chromophores [31] and agrochemicals [32]. To date, although several approaches have been reported for the synthesis

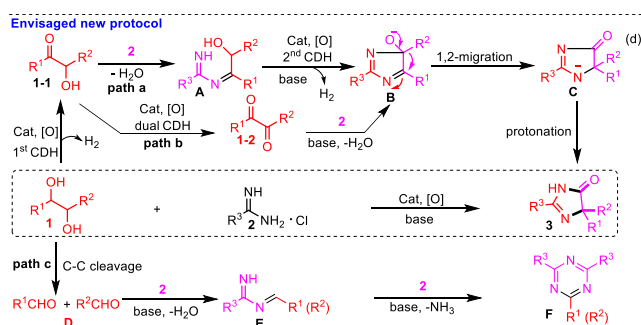
\* Corresponding author.

E-mail addresses: [xiefeng0401@126.com](mailto:xiefeng0401@126.com) (F. Xie), [minzhang@scut.edu.cn](mailto:minzhang@scut.edu.cn) (M. Zhang).

<sup>1</sup> F.X. and X.C. contributed equally to this work.



**Scheme 1.** Examples on the transformations of vicinal Diols to N-heterocycles.



**Scheme 2.** Envisaged new protocol.

of different substituted imidazolinones [33–35], these transformations generally suffer from one or more limitations such as the use of less environmentally benign agents, the need for prefunctionalization steps to access specific agents, and difficult catalyst reusability. In this context, the development of new strategies enabling efficient access to various imidazolinones, preferably with biomass-derived vicinal diols and reusable catalysts, would be highly desirable.

As a continuation of our efforts toward the construction/functionalization of N-heterocycles [36–39], we envisioned a new strategy for general synthesis of imidazolinone 3, that is, the combination of aerobic dehydrocyclization of vicinal diols 1 and amidines 2 with group migration. As illustrated in Scheme 2, the first catalytic dehydrogenation (1st CDH) of 1 under the assistance of nanocobalt and air (oxidant) forms hydroxyketone 1–1. Then, intermediate B is generated via the condensation of amidine 2 with 1–1 followed by the second catalytic dehydrogenation of A (2nd CDH) and base-mediated amino addition to the carbonyl group (path a). Alternatively, successive full catalytic dehydrogenation of diol 1, the capture of *in situ* formed dione 1–2 by amidine 2, and intramolecular cyclization also rationalize the formation of B (path b). Finally, the subsequent group 1,2-migration [33] and protonation of C give rise to the desired product 3. However, it is important to note that, under aerobic dehydrogenative and basic conditions, vicinal diols can easily undergo C–C bond cleavage to generate aldehydes D [40]. Moreover, the generated aldehydes D unavoidably react with two molecules of amidine 2 to form triazine by-products F (path c) [41–42]. Hence, to achieve a chemoselective synthesis of product 3, it is essential to find a compatible catalyst system to ensure that the dehydrogenated intermediate 1–1 or 1–2 is timely trapped by amidine 2, thus suppressing the decomposition of diols 1 to undesired aldehydes.

With the above information, we believe that the development of a suitable heterogeneous nanocatalyst would offer a solution to achieve the desired synthetic purpose (Scheme 2). In comparison with homogeneous catalysis, such type of catalyst has the

merits of regulable oxidative performance, intrinsic stability and easy recyclability. In recent years, OMS-2 has gained considerable attention [43–44], and the OMS-2 materials have exhibited attractive applications in selective oxidation due to the highly porous structure, controllable valence state and mobility of oxygen ions [45–46]. Moreover, cobalt-based nanocatalysts have greatly facilitated the advances of alcohol oxidation [47–48]. However, it is important to note that these examples are only confined to the well-known organic reactions, and their potentials in developing innovative organic transformations have been scarcely demonstrated. Herein, by developing an OMS-2 nanorod-supported cobalt catalyst, we wish to report, for the first time, its utility in efficient construction of imidazolinones via aerobic dehydrocyclization of vicinal diols with amidines.

## 2. Experimental

### 2.1. Synthesis of Co/OMS-2–800

Typically, the cobalt heterogeneous catalyst was prepared by pyrolysis of the cobalt hydroxide immobilized on the pre-synthesized OMS-2 materials [49–50]. Initially, the OMS-2 framework was obtained from the reaction of KMnO<sub>4</sub> and MnSO<sub>4</sub> with assistance of concentrated HNO<sub>3</sub>. After that, the *in situ* generated Co hydroxide was embedded and deposited into the cage of OMS-2 via impregnation method. Further, this supported hydroxide catalyst was pyrolyzed under argon flow at 800 °C for 4 h, which produced cobalt-doped octahedral molecular sieve (denoted as Co/OMS-2–800, for more details see the supporting information (SI)).

The crystal phase of the Co/OMS-2–800 has been analyzed by XRD (Figure S1 in the SI). The peaks at 12.7°, 18°, 28.9°, 37.2°, 42°, 50°, 56.1°, 60.1°, 69.4° are assignable to lattice planes of OMS-2, which is typical cryptomelane phase (JCPDS-00-020-0908) [46]. This result indicates that the crystal form of OMS-2 is retained even under high-temperature pyrolysis. Diffraction corresponding to CoO at 2θ = 36.4°, 42.4°, 61.5° were recognized with JCPDS (43–1004) [45]. Moreover, Peaks related to Co<sub>3</sub>O<sub>4</sub> (JCPDS-43–1003) were observed for a reflection at 2θ = 31.3°, 36.8°, 38.4°, 44.8°, 59.2°, 65.2° [45]. A typical IV isotherm with hysteresis loop arose in the N<sub>2</sub> adsorption–desorption isotherms of Co/OMS-2–800, which suggests a highly porous structure (SI, Figure S2). Notably, there is a dominant distribution of pore size centered at 2–4 nm, which makes for substrate diffusion.

The morphology and structural characterization of the prepared Co/OMS-2–800 material was investigated by means of TEM, STEM and EDS analyses. The TEM images (Fig. 1a-1b and Figure S3 (SI)) clearly demonstrate that the catalyst exists in the form of nanorods. The average diameter of the nanorods was in the range of 85–90 nm. As shown in HAADF-STEM image (Fig. 1c) and corresponding elemental mapping results (Fig. 1d-1f and Figure S4 (SI)), the impregnated Co was well dispersed over OMS-2 nanorods. Furthermore, the signals of Co, Mn, K, C, O are highly overlapped and interconnected with each other, which are surrounded by the carbon matrix. These results confirm that the Co species present uniform dispersion on the surface of OMS-2.

To identify the surface chemistry of the developed Co/OMS-2–800, the X-ray photoelectron spectroscopy (XPS) was then conducted. The element contents are as follows: Co (2.44 wt%), C (22.76 wt%), Mn (41.87 wt%), and O (32.93 wt%). Furthermore, the content of Co loading was determined by ICP-OES (2.1 wt%), which is very closely to the value detected by XPS (2.44 wt%). These results indicate the Co species supported on OMS-2 are highly uniform. The Co 2p spectrum (Figure S5a) shows characteristic peak of Co<sup>2+</sup> species with a binding energy of 780.6 eV [51–52],

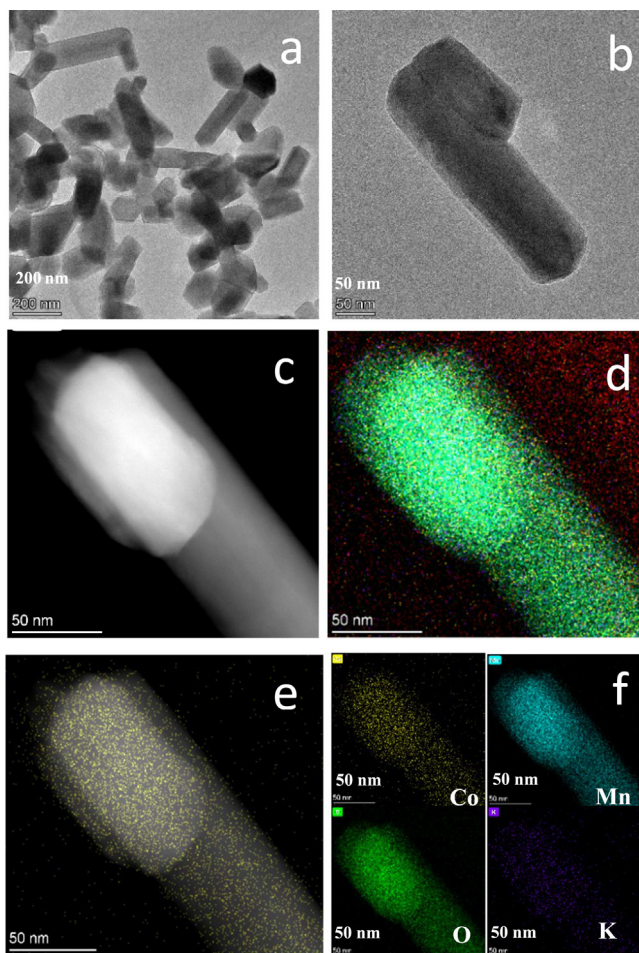


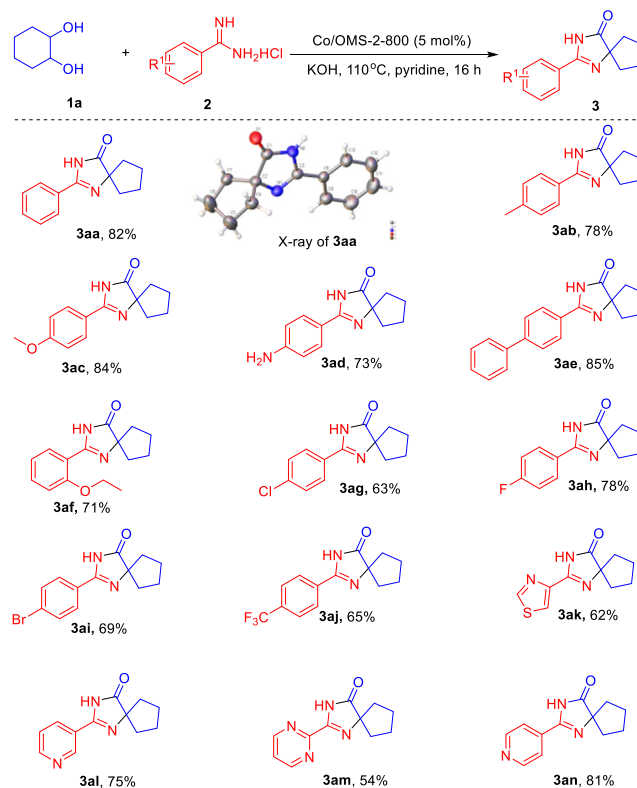
**Fig. 1.** (a–b) TEM images of Co/OMS-2-800. (c) HAADF-STEM image of Co/OMS-2-800 and corresponding EDS elemental maps (d). (e) HAADF image combined with elemental map of Co. (f) EDS elemental maps for Co, Mn, O, K.

the peak with typical binding energy of 795.8 eV of the Co 2p<sub>1/2</sub> electrons is attributed to Co<sub>3</sub>O<sub>4</sub> [53]. In agreement with XRD results, the XPS results suggest that the cobalt nanoparticles are cobalt oxides. In addition, The Mn 2p spectrum (Figure S5b) could be deconvoluted into three peaks with Mn<sup>2+</sup> (640.7 eV), Mn<sup>3+</sup> (642.2 eV), Mn<sup>4+</sup> (643.4 eV), respectively [46]. This unique mixed valence of Mn is beneficial to electron transport.

### 3. Catalytic performance.

To test the catalytic performance of the the prepared Co/OMS-2-800 material, we chose the dehydrogenative cyclization of 1,2-cyclohexanediol **1a** and benzamidine hydrochloride **2a** as a model reaction to evaluate different reaction parameters, including the effects of the catalysts, base additives, solvents, and temperatures (see Table S1 in the supporting information (SI)). An optimal GC yield (87%) of product **3aa** with spiro-structure was obtained at 110 °C by using 5 mol% of catalyst, air, KOH (2 equiv), and pyridine as the oxidant, base, and solvent, respectively.

With the optimal conditions (standard conditions) in hand, we then examined the generality of the synthetic protocol. Initially, the reaction of 1,2-cyclohexanediol **1a** with various amidines **2** (**2a–2n**, see Scheme S1 for their structures in SI) were explored. As presented in Scheme 3, all the reactions underwent smoothly and afforded the spirocyclic products in moderate to high yields (see **3aa–3an**). The structure of product **3aa** was identified by

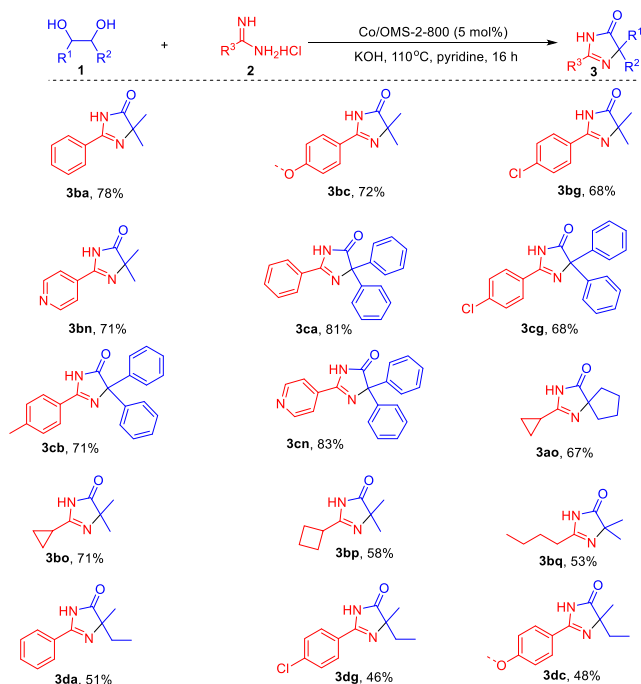


**Scheme 3.** Variation of amidines.

single-crystal X-ray diffraction (Scheme 3). Various functional groups (i.e., –Me, –OMe, –OC<sub>2</sub>H<sub>5</sub>, –NH<sub>2</sub>, –CF<sub>3</sub>, –F, –Cl and –Br) on the aryl ring of amidines **2** were well tolerated, these substituents with different electronic properties slightly affected the product yields. In general, the electron-donating groups (**3ab–3af**) afforded relatively higher yields than those strong electron-withdrawing ones (**3ag–3aj**). This phenomenon is accounted for the electron-rich substituents enhancing the reactivity of the –NH<sub>2</sub> group of amidines, thus favoring the condensation process (Scheme 2, from **1** to **1** or **1–2** to **B**). In addition, a series of heteroaromatic amidines **2** (**2 l–2n**) also effectively coupled with **1a** to afford the desired products (**3al–3an**) in moderate to good isolated yields, the success of these examples demonstrates the potential of the developed chemistry in further development of N-bidentate ligands (see **3ak** and **3am**).

Subsequently, we turned our attention to the transformation of various vicinal diols with different types of amidines (see Scheme S1 for their structures in SI). As shown in Scheme 4, all the substrates underwent efficient dehydrocyclization, affording the multisubstituted imidazolones in a regioselective manner. Similar to the results described in Scheme 3, electron-rich amidines gave the products (Scheme 4, **3bc**, **3cb**, **3dc**) in relatively higher yields than those of electron-poor ones (Scheme 4, **3bg**, **3cg**, **3dg**). Gratifyingly, among all halo-substituted substrates tested, no hydrodehalogenation was observed, indicating that the synthetic protocol has unique chemoselectivity. The retention of these functionalities offers the potential for the fabrication of complex products via further chemical transformations. In addition to aryl amidines, alkyl amidines (**2o–2q**) also underwent efficient oxidative dehydrocyclization, affording the alkylated products in moderate yields (**3ao–3bq**). Notably, unsymmetrical diol **1d** effectively coupled with different amidines and yielded the desired products in reasonable yields (**3da–3dc**).

To assess the stability and reusability of the catalyst material (Co/OMS-2-800), the model reaction was performed in five con-



Scheme 4. Variation of Both Coupling Partners.

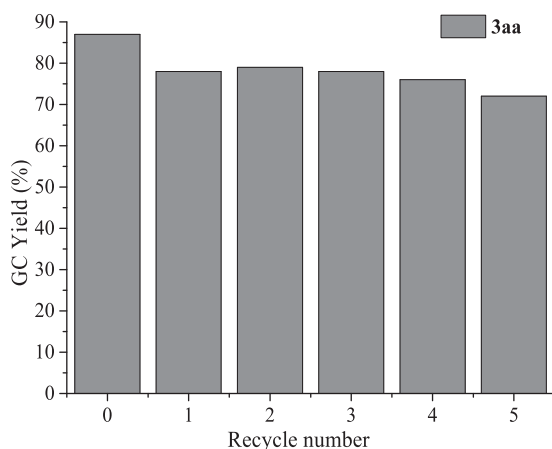
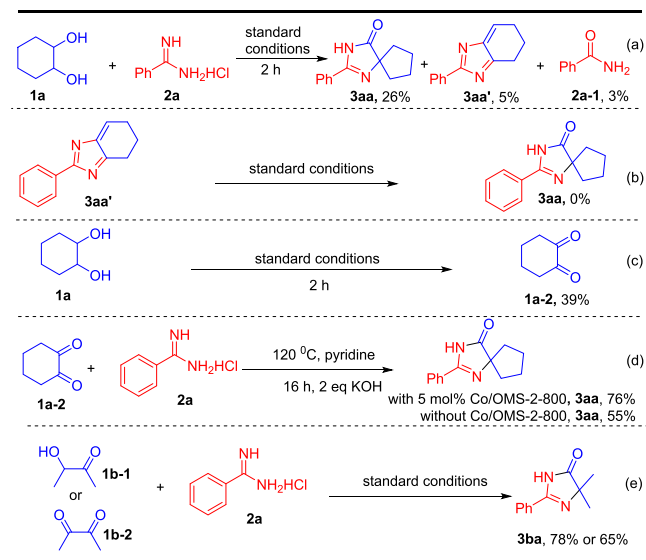


Fig. 2. Reuse of the Co/OMS-2-800 catalysts.

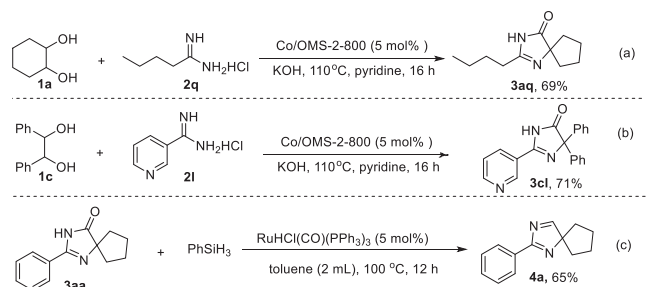
secutive runs. As illustrated in Fig. 2, the catalytic activity still maintained very well, only with a slight decline of yields, demonstrating high stability of the developed catalyst. Meanwhile, the Co content of reused Co/OMS-2-800 was determined by ICP-AES (1.9 wt%), which are closely to the Co content of fresh catalyst. In addition, the HRTEM images (Figure S3e–3f, SI) of the reused catalyst show that there are no obvious Co cluster aggregation during the reaction and the morphology of catalyst is preserved very well. The reason for slight reduction of yield is ascribed to slight loss of Co during the recycling and mechanical abrasion.

#### 4. Mechanistic insights

To gain insight into the reaction mechanism, several control experiments were performed (Scheme 5). First, the model reaction was terminated after 2 h to analyze the product system. In addition to the spirocyclic product 3aa detected in 26% yield, by-product benzamide 2a-1 and imidazole derivative 3aa', deriving from the



Scheme 5. Control Experiments.



Scheme 6. Synthetic Utilit.

hydrolysis of 2a and dehydrogenative condensation of substrates 1a and 2a, were isolated in 3% and 5% yields, respectively (Scheme 5a). Meanwhile, the time-yield profile of the model reaction was depicted in Figure S6, the desired product 3aa accumulated to a maximum content within 16 h, and very low yields of compounds 3aa' and 2a-1 were observed after completion of the reaction and they can not be transformed into product 3aa (Scheme 5b), indicating 3aa' and 2a-1 are the by-products and the reaction offers high chemoselectivity. Furthermore, subsection of 1,2-cyclohexanediol 1a under the standard conditions for 2 h generated 1, 2-cyclohexanedione 1a-2 in 39% yield (Scheme 5c). Noteworthy, as shown in Figure S8 using methane as the internal standard, we have detected the generation of H<sub>2</sub> during the reaction. The reaction of 1a-2 and 2a under standard conditions afforded product 3aa in high yield, whereas the coupling of 1a-2 and 2a without catalyst gave product 3aa in 55% yield (Scheme 5d), which showed that the use of our newly developed catalyst significantly improve the product yield. The reaction of hydroxyketone 1b-1 or diketone 1b-2 with 2a also gave product 3ba in high yields (Scheme 5e), indicating that 1b-1 and 1b-2 serve as the reaction intermediates. All these results are in good agreement with the pathway proposed in Scheme 2.

Next, we were interested in exploring the synthetic utility of the newly developed chemistry. First, the reaction of 1a and 2q furnished the desired product 3aq in 69% yield (Scheme 6a), a key precursor employed for the preparation of antihypertensive drug Avapro [54]. In addition, the reaction of 1c and 2l produced 5,5-diphenylimidazolone 3cl in 71% yield (Scheme 6b), which is used

as a potent antagonist for human neuropeptide Y5 receptor [29]. Finally, selective hydrosilylation of compound **3aa** afforded product **4a** in 65% yield without reduction of the C = N bond in the presence of RuHCl(CO)(PPh<sub>3</sub>)<sub>3</sub> catalyst and silane reductant (Scheme 6c).

In summary, by developing a highly dispersed OMS-2 nanorod-supported cobalt catalyst, we have successfully applied it to develop a new aerobic dehydrocyclization reaction of vicinal diols and amidines, offering an efficient way to access structurally diverse imidazolone derivatives. The catalytic transformation proceeds with broad substrate scope and good functional group compatibility, uses molecular oxygen in the air as the green oxidant and reusable base-metal as the catalyst, and is highly chemoselective and atom-efficient. The work presented offers a practical platform for further discovery of functional products including biologically and pharmaceutically active molecules, and the strategy combining nanocatalyst design with aerobic dehydrocoupling is anticipated to achieve more challenging but valuable synthetic purposes.

### Declaration of Competing Interest

All the authors declare that we have no financial and personal relationship with people and organizations that can inappropriately influence our work, there is no professional or other personal interest of any nature or kind in any product, service and/or company that could be construed as influencing the position presented in, or the review of, the manuscript entitled.

### Acknowledgements

We thank the Department of Education of Guangdong province (2019KZDXM052, 2020KQNCX093), the Science Foundation for Young Teachers of Wuyi University (2019td06), the Innovation Industry Project of Wuyi University (2019CX24, 202011349025), “Climbing Program” Special Funds of Guangdong Province (pdjh2021b0516), and National Natural Science Foundation of China (21971071) for financial support. The authors thank Shiyanjia Lab (www.shiyanjia.com) for the support of XPS and TEM test as well.

### Appendix A. Supplementary data

Supplementary data to this article can be found online at <https://doi.org/10.1016/j.jcat.2021.04.022>.

### References

- [1] S.A. Akhade, N. Singh, O.Y. Gutiérrez, J. Lopez-Ruiz, H. Wang, J.D. Holladay, Y. Liu, A. Karkamkar, R.S. Weber, A.B. Padmaperuma, M.-S. Lee, G.A. Whyatt, M. Elliott, J.E. Holladay, J.L. Male, J.A. Lercher, R. Rousseau, V.-A. Glezakou, Electrocatalytic Hydrogenation of Biomass-Derived Organics: A Review, *Chem. Rev.* 120 (2020) 11370–11419.
- [2] R. Gérardy, D.P. Debecker, J. Estager, P. Luis, J.-C.-M. Monbaliu, Continuous Flow Upgrading of Selected C2–C6 Platform Chemicals Derived from Biomass, *Chem. Rev.* 120 (2020) 7219–7347.
- [3] S. Michlik, R. Kempe, A sustainable catalytic pyrrole synthesis, *Nat. Chem.* 5 (2013) 140–144.
- [4] K.A. Goulas, A.A. Gokhale, Kinetics of the Homogeneous and Heterogeneous Coupling of Furfural with Biomass-Derived Alcohols, *ChemCatChem* 10 (2018) 2387–2393.
- [5] L. Wu, T. Moteki, A.A. Gokhale, D.W. Flaherty, F.D. Toste, Production of Fuels and Chemicals from Biomass, Condensation Reactions and Beyond, *Chem* 1 (2016) 32–58.
- [6] M. Liu, C.-J. Li, C-C Oxidative Cleavage in the Aerobic Esterification of Alcohol, *Chem* 6 (2020) 3163–3165.
- [7] Z. Shao, Y. Li, C. Liu, W. Ai, S.-P. Luo, Q. Liu, Reversible interconversion between methanol-diamine and diamide for hydrogen storage based on manganese catalyzed (de)hydrogenation, *Nat. Commun.* 11 (2020) 591.
- [8] Y.-Q. Zou, Q.-Q. Zhou, Y. Diskin-Posner, Y. Ben-David, D. Milstein, Synthesis of oxalamides by acceptorless dehydrogenative coupling of ethylene glycol and amines and the reverse hydrogenation catalyzed by ruthenium, *Chem. Sci.* 11 (2020) 7188–7193.
- [9] S. Bera, A. Bera, D. Banerjee, Nickel-catalyzed hydrogen-borrowing strategy: chemo-selective alkylation of nitriles with alcohols, *Chem. Commun.* 56 (2020) 6850–6853.
- [10] M. Mastalir, M. Glatz, E. Pittenauer, G. Allmaier, K. Kirchner, Ruthenium-Catalyzed Dehydrogenative Coupling of Alcohols and Amines to Afford Nitrogen-Containing Aromatics and More, *Org. Lett.* 21 (2019) 1116–1120.
- [11] L.J. Donnelly, S.P. Thomas, J.B. Love, Recent Advances in the Deoxydehydration of Vicinal Diols and Polyols, *Chem. Asian J.* 14 (2019) 3782–3790.
- [12] T. Irrgang, R. Kempe, 3d-Metal Catalyzed N- and C-Alkylation Reactions via Borrowing Hydrogen or Hydrogen Autotransfer, *Chem. Rev.* 119 (2019) 2524–2549.
- [13] M. Vellakkaran, K. Singh, D. Banerjee, An Efficient and Selective Nickel-Catalyzed Direct N-Alkylation of Anilines with Alcohols, *ACS Catal.* 7 (2017) 8152–8158.
- [14] W. Hu, Y. Zhang, H. Zhu, D. Ye, D. Wang, Unsymmetrical triazolyl-naphthyridinyl-pyridine bridged highly active copper complexes supported on reduced graphene oxide and their application in water, *Green Chem.* 21 (2019) 5345–5351.
- [15] R. Tao, Y. Yang, H. Zhu, X. Hu, D. Wang, Ligand-tuned cobalt-containing coordination polymers and applications in water, *Green Chem.* 22 (2020) 8452–8461.
- [16] W. Yao, Y. Zhang, H. Zhu, C. Ge, D. Wang, The synthesis and structure of pyridine-oxadiazole iridium complexes and catalytic applications: Non-coordinating-anion-tuned selective CN bond formation, *Chinese Chem. Lett.* 31 (2020) 701–705.
- [17] Z.-Z. Zhou, M. Liu, L. Lv, C.-J. Li, Silver(I)-Catalyzed Widely Applicable Aerobic 1,2-Diol Oxidative Cleavage, *Angew. Chem. Int. Ed.* 57 (2018) 2616–2620.
- [18] R.D. Hancock, The pyridyl group in ligand design for selective metal ion complexation and sensing, *Chem. Soc. Rev.* 42 (2013) 1500–1524.
- [19] D.-S. Wang, Q.-A. Chen, S.-M. Lu, Y.-G. Zhou, Asymmetric Hydrogenation of Heteroarenes and Arenes, *Chem. Rev.* 112 (2012) 2557–2590.
- [20] C. Beemelmans, H.-U. Reissig, Samarium diiodide induced ketyl-(het)arene cyclisations towards novel N-heterocycles, *Chem. Soc. Rev.* 40 (2011) 2199–2210.
- [21] M. Peña-López, H. Neumann, M. Beller, (Enantio)selective Hydrogen Autotransfer: Ruthenium-Catalyzed Synthesis of Oxazolidin-2-ones from Urea and Diols, *Angew. Chem. Int. Ed.* 55 (2016) 7826–7830.
- [22] M. Zhang, X. Fang, H. Neumann, M. Beller, General and Regioselective Synthesis of Pyrroles via Ruthenium-Catalyzed Multicomponent Reactions, *J. Am. Chem. Soc.* 135 (2013) 11384–11388.
- [23] T. Hille, T. Irrgang, R. Kempe, The Synthesis of Benzimidazoles and Quinoxalines from Aromatic Diamines and Alcohols by Iridium-Catalyzed Acceptorless Dehydrogenative Alkylation, *Chem. Eur. J.* 20 (2014) 5569–5572.
- [24] P. Daw, Y. Ben-David, D. Milstein, Acceptorless Dehydrogenative Coupling Using Ammonia: Direct Synthesis of N-Heteroaromatics from Diols Catalyzed by Ruthenium, *J. Am. Chem. Soc.* 140 (2018) 11931–11934.
- [25] P. Daw, A. Kumar, N.A. Espinosa-Jalapa, Y. Diskin-Posner, Y. Ben-David, D. Milstein, Synthesis of Pyrazines and Quinoxalines via Acceptorless Dehydrogenative Coupling Routes Catalyzed by Manganese Pincer Complexes, *ACS Catal.* 8 (2018) 7734–7741.
- [26] T. Hille, T. Irrgang, R. Kempe, Synthesis of meta-Functionalized Pyridines by Selective Dehydrogenative Heterocondensation of β- and γ-Amino Alcohols, *Angew. Chem. Int. Ed.* 56 (2017) 371–374.
- [27] X. Bao, W. Zhu, W. Yuan, X. Zhu, Y. Yan, H. Tang, Z. Chen, Design, synthesis and evaluation of novel potent angiotensin II receptor 1 antagonists, *Eur. J. Med. Chem.* 123 (2016) 115–127.
- [28] T. Lu, C. Schubert, M.D. Cummings, G. Bignan, P.J. Connolly, K. Smans, D. Ludovici, M.H. Parker, C. Meyer, C. Rocaboy, R. Alexander, B. Grasberger, S. De Breucker, N. Esser, E. Fraiponts, R. Gilissen, B. Janssens, D. Peeters, L. Van Nuffel, P. Vermeulen, J. Bischoff, L. Meerpoel, Design and synthesis of a series of bioavailable fatty acid synthase (FASN) KR domain inhibitors for cancer therapy, *Bioorg. Med. Chem.* 28 (2018) 2159–2164.
- [29] K.W. Gillman, M.A. Higgins, G.S. Poindexter, M. Browning, W.J. Clarke, S. Flowers, J.E. Grace, J.B. Hogan, R.T. McGovern, L.G. Iben, G.K. Mattson, A. Ortiz, S. Rassnick, J.W. Russell, I. Antal-Zimanyi, Synthesis and evaluation of 5,5-diphenylimidazolones as potent human neuropeptide Y5 receptor antagonists, *Bioorg. Med. Chem.* 14 (2006) 5517–5526.
- [30] Y.-C. Hu, C.-F. Liang, J.-H. Tsai, G.P.A. Yap, Y.-T. Chang, T.-G. Ong, Zirconium Complexes Supported by Imidazolones: Synthesis, Characterization, and Application of Precatalysts for the Hydroamination of Aminoalkenes, *Organometallics* 29 (2010) 3357–3361.
- [31] E.A. Dolgoplova, A.A. Berseneva, M.S. Faillace, O.A. Ejegbavwo, G.A. Leith, S.W. Choi, H.N. Gregory, A.M. Rice, M.D. Smith, M. Chruszcz, S. Garashchuk, K. Myhre, N.B. Shustova, Confinement-Driven Photophysics in Cages, Covalent–Organic Frameworks, Metal–Organic Frameworks, and DNA, *J. Am. Chem. Soc.* 142 (2020) 4769–4783.
- [32] Y. Kacem, B. Ben Hassine, Solvent-free synthesis of new chiral 3-phenylamino-3,5-dihydro-4H-imidazol-4-one derivatives from α-amino acid phenylhydrazides, *Heterocycles* 89 (2014) 197–207.
- [33] C. Zhu, C. Liu, H. Zeng, F. Chen, H. Jiang, Transition-metal free selective C(α)–C(β) bond cleavage of trifluoromethyl ketones with amidines under air: facile access to 5-trifluoromethylated Imidazol-4-ones, *Org. Chem. Front.* 6 (2019) 858–862.

- [34] Y. Xie, X. Cheng, S. Liu, H. Chen, W. Zhou, L. Yang, G.-J. Deng, Efficient 4,5-dihydro-1H-imidazol-5-one formation from amidines and ketones under transition-metal free conditions, *Green Chem.* 17 (2015) 209–213.
- [35] A. Clemenceau, Q. Wang, J. Zhu, Cooperative Pd/Cu Catalysis: Multicomponent Synthesis of Tetrasubstituted Imidazolones from Methyl  $\alpha$ -Isocyanoacetates, Primary Amines, and Aryl(vinyl) Iodides, *Org. Lett.* 20 (2018) 126–129.
- [36] R. Xie, F. Xie, C.-J. Zhou, H.-F. Jiang, M. Zhang, Hydrogen transfer-mediated selective dual C-H alkylations of 2-alkylquinolines by doped TiO<sub>2</sub>-supported nanocobalt oxides, *J. Catal.* 377 (2019) 449–454.
- [37] T. Liang, Z. Tan, H. Zhao, X. Chen, H. Jiang, M. Zhang, Aerobic Copper-Catalyzed Synthesis of Benzimidazoles from Diaryl- and Alkylamines via Tandem Triple C-H Aminations, *ACS Catal.* 8 (2018) 2242–2246.
- [38] F. Xie, M. Zhang, H. Jiang, M. Chen, W. Lv, A. Zheng, X. Jian, Efficient synthesis of quinoxalines from 2-nitroanilines and vicinal diols via a ruthenium-catalyzed hydrogen transfer strategy, *Green Chem.* 17 (2015) 279–284.
- [39] X.-W. Chen, H. Zhao, C.-L. Chen, H.-F. Jiang, M. Zhang, Hydrogen-Transfer-Mediated  $\alpha$ -Functionalization of 1,8-Naphthyridines by a Strategy Overcoming the Over-Hydrogenation Barrier, *Angew. Chem. Int. Ed* 56 (2017) 14232–14236.
- [40] B. Guichet, E. Da Silva, R. Philippe, A. Favre-Reguillon, L. Vanoye, P. Blach, Y. Raoul, C. De Bellefon, E. Méty, M. Lemaire, Aerobic Oxidative Cleavage of Vicinal Diol Fatty Esters by a Supported Ruthenium Hydroxide Catalyst, *ACS Sustain. Chem. Eng.* 8 (2020) 13167–13175.
- [41] W. Guo, M. Zhao, W. Tan, L. Zheng, K. Tao, X. Fan, Developments towards synthesis of N-heterocycles from amidines via C-N/C-C bond formation, *Org. Chem. Front.* 6 (2019) 2120–2141.
- [42] F. Xie, M. Chen, X. Wang, H. Jiang, M. Zhang, An efficient ruthenium-catalyzed dehydrogenative synthesis of 2,4,6-triaryl-1,3,5-triazines from aryl methanols and amidines, *Org. Biomol. Chem.* 12 (2014) 2761–2768.
- [43] A. Iyer, C.-H. Kuo, S. Dharmarathna, Z. Luo, D. Rathnayake, J. He, S.L. Suib, An ultrasonic atomization assisted synthesis of self-assembled manganese oxide octahedral molecular sieve nanostructures and their application in catalysis and water treatment, *Nanoscale* 9 (2017) 5009–5018.
- [44] D.S. Pisal, G.D. Yadav, Synthesis of salicylaldehyde through oxidation of o-cresol: Evaluation of activity and selectivity of different metals supported on OMS-2 nanorods and kinetics, *Mol. Catal.* 491 (2020) 110991.
- [45] Y. Hao, L. Li, Z. Lu, X. Yu, X. Zhang, X. Yang, OMS-2 nanorods filled with Co-ion in the tunnels as efficient electron conduits and regulatory substance for oxygen reduction, *Appl. Catal. B: Environ.* 279 (2020) 119373.
- [46] Y. Huang, Y. Wang, X. Meng, X. Liu, Highly efficient Co-OMS-2 catalyst for the degradation of reactive blue 19 in aqueous solution, *Inorg. Chem. Commun.* 112 (2020) 107757.
- [47] J. Li, G. Liu, X. Long, G. Gao, J. Wu, F. Li, Different active sites in a bifunctional Co@N-doped graphene shells based catalyst for the oxidative dehydrogenation and hydrogenation reactions, *J. Catal.* 355 (2017) 53–62.
- [48] R.V. Jagadeesh, H. Junge, M.-M. Pohl, J. Radnik, A. Brückner, M. Beller, Selective Oxidation of Alcohols to Esters Using Heterogeneous Co<sub>3</sub>O<sub>4</sub>-N@C Catalysts under Mild Conditions, *J. Am. Chem. Soc.* 135 (2013) 10776–10782.
- [49] K. Yamaguchi, H. Kobayashi, Y. Wang, T. Oishi, Y. Ogasawara, N. Mizuno, Green oxidative synthesis of primary amides from primary alcohols or aldehydes catalyzed by a cryptomelane-type manganese oxide-based octahedral molecular sieve, OMS-2, *Catal. Sci. Technol.* 3 (2013) 318–327.
- [50] K. Yamaguchi, Y. Wang, T. Oishi, Y. Kuroda, N. Mizuno, Heterogeneously Catalyzed Aerobic Cross-Dehydrogenative Coupling of Terminal Alkynes and Monohydrosilanes by Gold Supported on OMS-2, *Angew. Chem. Int. Ed.* 52 (2013) 5627–5630.
- [51] F. Xie, G.-P. Lu, R. Xie, Q.-H. Chen, H.-F. Jiang, M. Zhang, MOF-Derived Subnanometer Cobalt Catalyst for Selective C-H Oxidative Sulfonylation of Tetrahydroquinoxalines with Sodium Sulfonates, *ACS Catal.* 9 (2019) 2718–2724.
- [52] R. Xie, G.-P. Lu, H.-F. Jiang, M. Zhang, Selective reductive annulation reaction for direct synthesis of functionalized quinolines by a cobalt nanocatalyst, *J. Catal.* 383 (2020) 239–243.
- [53] F. Xie, R. Xie, J.-X. Zhang, H.-F. Jiang, L. Du, M. Zhang, Direct Reductive Quinoyl  $\beta$ -C-H Alkylation by Multispherical Cavity Carbon-Supported Cobalt Oxide Nanocatalysts, *ACS Catal.* 7 (2017) 4780–4785.
- [54] M. Adib, M. Mahdavi, A. Abbasi, A.H. Jahromi, H.R. Bijanzadeh, Efficient synthesis of imidazo[1,2-a]pyridin-3(2H)-ones, *Tetrahedron Lett.* 48 (2007) 3217–3220.